IAES International Journal of Artificial Intelligence (IJ-AI)
Vol. 12, No. 4, December 2023, pp. 2011~2021
ISSN: 2252-8938, DOI: 10.11591/ijai.v12.i4.pp2011-2021

Automated classification of age-related macular degeneration from optical coherence tomography images using deep learning approach

Gilakara Muni Nagamani, Theerthagiri Sudhakar
School of Computer Science and Engineering, VIT-AP University, Amaravati, Andhra Pradesh, India

Article Info

Article history:

Received Oct 26, 2022
Revised Feb 1, 2023
Accepted Mar 10, 2023

Keywords:

Image classification automated
Diagnosis choroidal
Neovascularization
Macular pathologies
Drusens

ABSTRACT

Early detection of macular diseases can prevent vision loss. Manual screening can be unreliable due to the similarity in the pathological presentations of common retinal illnesses like age-related macular degeneration (AMD). Researchers are becoming more interested in the accurate automated computer-based detection of macular diseases. Using healthy optical coherence tomography (OCT) images, the drusens (early stage) and choroidal neovascularization (CNV) (late stage) of AMD are thus classified using a completely different approach in this paper. The new deep learning (DL) model is proposed for multiple OCT image segmentation of ophthalmological diseases using attention-based nested U-Net (ANU-Net). The flower pollination optimization algorithm (FPOA) is used to optimize the hyperparameters of the network. The SqueezeNet-based classification can be made in the pre-processed images. A dataset from the University of California San Diego (UCSD) is used to evaluate the proposed method. 98.7% accuracy, 99.8% specificity, and 99.7% sensitivity are achieved by the proposed method. The proposed method produces better identification results for automated preliminary diagnosis of macular diseases in hospitals and eye clinics due to the positive classification results.

Corresponding Author:

Theerthagiri Sudhakar
Associate Professor, School of Computer Science and Engineering, VIT-AP University
Amaravati, Andhra Pradesh, India.
Email: drsudhakar.vitap@gmail.com

1. INTRODUCTION

Nearly 8% of people worldwide are affected by macular diseases such as age-related macular degeneration (AMD) and diabetic macular edema (DME), which are widespread retinal problems [1]. The WHO has classified AMD, the frequent leading cause of blindness in the elderly, as a priority eye disease. On the other hand, DME is a side effect of diabetes [2]. In people with diabetes, DME is the main factor contributing to visual loss and blindness [3]. Leaving it untreated for a year or more can result in significant vision loss [4]. For diagnosing specific diseases, scientists were forced to develop an advanced and effective technique in these situations [5]. Optical coherence tomography (OCT) images is a type of imaging technology [6]. The incoming weak coherent light is detected by its back reflection and detects multiple scattered signals at various biological tissue levels [7]. As a result, scanning can obtain cellular tissues with representations of their structural details in two or three dimensions, which displays cross-sectional images similar to ultrasonography [8]. Computers can now learn how to analyze medical images when new learning algorithms are developed [9], [10].

This concept has led to the development of numerous deep-learning network models composed of multiple layers that classify raw images while learning ever-deeper traits [11]. The most commonly used deep learning method for diagnosing medical diseases is the convolutional neural network (CNN) technology, especially for data based on OCT images [12]. A minimum number of layers in CNN's network use the convolutional layer to transform their input [13]. Although deep learning has revolutionized computer vision, its implementation still needs to be improved due to the scarcity of large training sets [14]. Before deep understanding can be employed efficiently, it is always necessary to offer a significant training set [15]. Fine vision, the ability to recognize colors, and other visual abilities are all characteristics of the retina's macular region, which is an essential part of the retina [16]. Adverse effects on vision will result from a lesion in the macular area [17].

Most persons over 45 suffer from macular disease (MD), which is the aging process in the region of macular. The first major causes of vision impairment is AMD due to the age-related increase in incidence rate [18]. In 2016, there were 170 million AMD sufferers worldwide. By 2040, it is expected that there will be 288 million cases worldwide. Neovascular (wet) AMD or regional atrophy (late dry) AMD are the two states in which the disorder evolves. The lipids, liquids, and blood are released by dividing the choroidal neovascularization (CNV) by the neural retina through the neovascular AMD. The most severe AMD vision loss is caused by these extreme forms of illness. As a result, an essential part of AMD treatment is early identification [19]. The nine retinal layers can be seen clearly by OCT. Its abnormalities and different thicknesses contain a wealth of information that can be used to identify disorders. There are two types of AMD: dry AMD (drusen) and wet AMD (CNV) [20].

Drusen, also known as dry AMD, is made up of tiny hyaline deposits with defined borders and is categorized as a complex formation by histology. It is thought to be an age-related low-risk change. Wet AMD, also known as CNV, the growth of new blood vessels is one of its characteristics. This study proposes a new deep learning-based approach for precise analysis and the capability of localizing retinal disorders. The main contribution of the model is:

- The retina's natural curvature is first removed during the pre-processing stage using a method of graph-based curvature removal, then the regions of interest are cropped.
- After completing a pre-processing phase, the deep learning-based SqueezeNet is used for adequate classification. The proposed framework is created for CNV and drusen classification in OCT images.
- The macular pathologies are accurately segmented by the proposed Attention based nested U-Net (ANU-Net). The proposed ANU-net performs the segmentation in each stage using multi-stage architecture and attention blocks. The CNN hyperparameters are optimized by using the flower pollination optimization algorithm (FPOA), and this optimization is used for increasing the classification performance.
- The proposed model evaluation uses the University of California San Diego (UCSD) database. Python is the platform used for experiments. It's employed to compare and contrast the proposed and existing methods. The proposed model's accuracy is better than the previous models.

The remainder of this work is arranged in the following manner. Section 2 introduces some relevant work related to the proposed segmentation method. The proposed methodology process is defined in section 3. Section 4 contains the experimental results & discussions. Section 5 concludes the paper.

2. LITERATURE REVIEW

Review various existing DL methods for diagnosing macular diseases in this section.

Thomas *et al.* [21] proposed an accurate AMD diagnosis using a new multipath CNN model. The regular and AMD images are classified using multipath CNN with five convolutional layers in the proposed model. Several global structures with a large filter kernel are generated by the multipath convolution layer. The classifier in this proposed network is the sigmoid function. Four widespread deep-learning models are examined by Alsaih *et al.* [22]. The retouch challenge data produced dense predictions while segmenting three retinal fluids. This paper shows how the patch-based approach improves each method's performance is indicated. For generalizing network performance, the optima challenge dataset is used for evaluating the proposed model. There are two sections to the analysis: the evaluation of the four methods and the significance of image patching.

Tan *et al.* [23] proposed a fourteen-layer deep CNN model for effectively detecting AMD at an early stage. The ten-fold and blindfold cross-validation processes evaluate the proposed model's performance. For the quick identification of AMD in elderly individuals, this innovative model can be used. Thus, the diagnosis using fundus images does not require any manufactured features. This proposed computer aided diagnostic (CAD) system for AMD can be used as a second opinion tool to assist ophthalmologists in their diagnosis.

A new model is proposed by Serener and Serte [24] for efficiently and automatically classifying dry and wet AMD. In this paper, deep CNN is used for the classification process. AlexNet and ResNet, deep CNN

networks, are used for disease classification. To receive timely treatment, it is essential to identify dry and wet types accurately. This paper demonstrates that dry vision impairment can be identified more precisely than wet vision impairment using the profound neural network performance results.

Karri *et al*. [25] presented an algorithm using OCT images for retinal pathologies detection. The prediction capability is improved by fine-tuning the pre-trained CNN and GoogLeNet while comparing them to the random initialization training. The salient responses are identified by this method for understanding the learned filter characteristics.

3. PROPOSED METHODOLOGY

3.1. Problem statement

The use of various deep-learning techniques in medical diagnostics is prevalent and successful. The same is true when applying them to the retina OCT sector, but i) medical researchers are unable to fully trust the results produced by these approaches because of their black box features ii) these techniques are limited in their application in medical and complex settings due to their lack of precision iii) in real-time applications, the classifier performance is decreased by the existing research and models on OCT image classification. These models are excessively complex and extensive, and also these models need a significant amount of computational power and memory. This research proposes a novel effective deep learning-based ANU-Net model for solving these problems.

3.2. Methodology

The automated AMD segmentation and classification are improved by employing several classification enhancement methods through an experimental evaluation. This is the real aim of this research. Three steps are used for the implementation of the proposed method. Using a graph-based curvature removal method, the retina's natural curvature is first removed during the pre-processing stage, then the regions of interest are cropped. After pre-processing, the classification is performed. The obtained pre-processed images are sent into the deep learning classifier SqueezeNet. After classification, whether the OCT images are typical or have CNV and drusen disorders is determined. Then proposed, an ANU-Net for segmenting the OCT images. The FPOA optimizer optimizes the hypermeters. The schematic diagram of the proposed method is given in Figure 1.

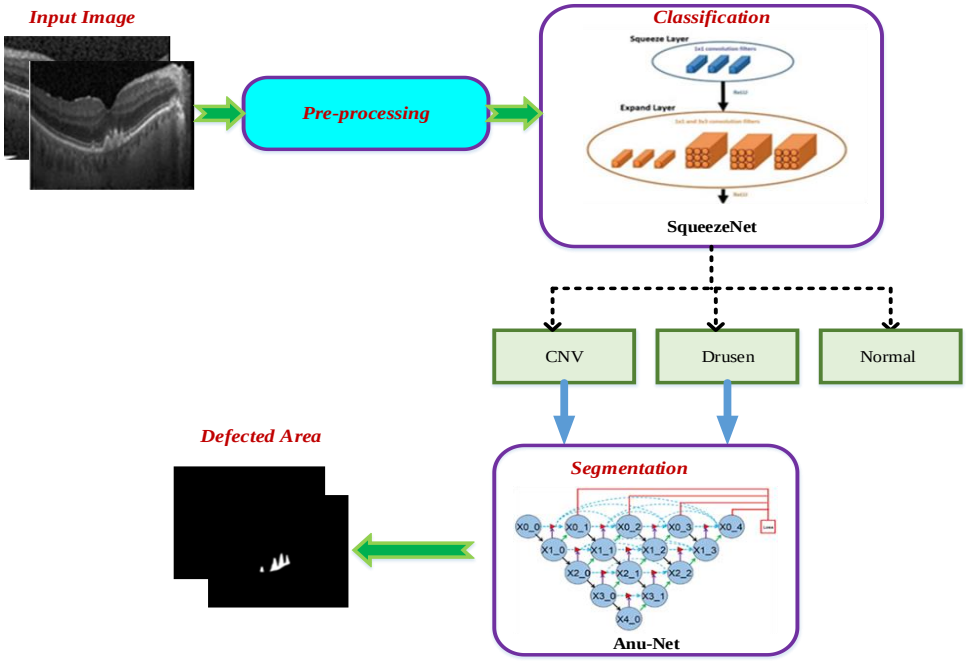

Figure 1. Schematic diagram of the proposed model

3.3. Database description

The UCSD database is used to assess the proposed method. This database presents four categories of OCT images: standard, drusen, DME, and CNV, for training and testing purposes. The training set has 83,484

OCT images total, with 26,315 healthy control images, 8,616 drusen images, 37,205 CNV images, and 11,348 DME images. One thousand images are presented in a test set from 633 patients. Patients from different ethnic backgrounds and age groups, both men and women, are included in the database. The normal, drusen, and CNV OCT images are classified by designing the proposed model. For the proposed model training, 80% of the training set's pictures and 20% of the test set's images were used.

3.4. Pre-processing

Different spatial resolution OCT images are presented in the dataset. The uniform field of vision is maintained by resizing the images into 496×512. Each patient's natural retinal curvature is different in the OCT images. Retinal flattening is used to reduce the classifier's sensitivity to retinal curvature. The image flattening approach is used in this work. Retinal pigment epithelium estimation (RPE) is the first step in flattening. Since the layer of the retina is the most hyper-reflective RPE, it can be approximated by locating the pixels in the B-brightest scan column. The retrieved locations are fitted with a second-order polynomial. In every B-scan column, a flat RPE brightest pixel is obtained by shifting each image column up or down.

The retinal layers are the only parts of the OCT images that contain diagnostic information. The choroid-sclera and vitreous are removed by cropping each B-scan horizontally with 90 pixels below and 160 pixels above the RPE. For further processing, scaling the OCT B-scans to 128×256. The interpatient variabilities are removed by normalizing B-scans for having unit standard deviation and zero means.

3.5. Classification using Squeeze-Net

The SqueezeNet convolutional network is used throughout the training and optimization phases. The input for testing is the test set. The information for testing is the test set. The SqueezeNet convolution network is used in the training and optimization stages, and a more effective and straightforward CNN architecture is constructed by squeezing and expanding the layers of the fire modules during training. The most effective network model is used to determine the classification performance of the infection classes.

The fifteen layers are presented in the SqueezeNet structure, including three max-pooling layers, one global average pooling layer, two convolution layers, one softmax output layer, and eight fire layers. The network's input has RGB channels and is 227×227 in size. Convolution is used to generalize the input images and apply the maximum pooling. The small regions and weights in the input volumes are convoluted by the convolution layer, which uses 3×3 kernels.

SqueezeNet uses the fire between the convolution layers, which comprises squeeze and expansion phases. The fire has a consistent input and output tensor scale. The 3×3 and 1×1 size filters are used in the expansion phase, while the 1×1 size filter is used in the squeeze phase. At first, the squeeze transmits the input tensor H×W×C. The ReLu units are involved in both the squeezing and extension phases. The squeeze operation compresses the depth, and the depth is increased by the expansion. The concatenate action is used to layering the expansion outputs in the input tensor's depth dimension. Assume the channel (C) and feature maps (FM), the squeeze operation's output layer f{y}, w can be represented as with the kernel, i.e.,

$$f\{y\} = \sum_{fm1=1}^{FM} \sum_{c=1}^{c} w_c^f \, x_c^{fm1} \quad (1)$$

Here, $f\{y\} \in R^N$ and$w \in R^{c\times 1\times FM2}$. The squeeze outputs define a weighted combination of the different tensors' feature maps. The max pool layers execute a down-sampling operation in the network along the spatial dimensions. The global average pool converts the class maps with features into one value. The softmax activation function towards the end of the network generates the multi-class probability distributions.

3.6. Segmentation using ANU-Net

An integrated network is developed for OCT image segmentation called Attention U-Net++. Nested U-Net design. Because nested convolutional blocks are generated by U-Net and between the decoder and encoder, it creates dense skip links at different depths. While compared to U-net, the nested model is very effective for segmentation. The semantic information is captured by every nested convolutional block using several convolutional layers in layered U-Nets. The concatenation layer combines different levels of semantic information, which is done by the connections between each layer in the block. The advantages of the new nested design are as follows: different depth features are considered separately.

- By determining the different depth features considered separately, the nested design may bypass the tedious process of selecting deep and shallow features.
- Since in the proposed hybrid network, the U-Nets share a feature extractor, only an encoder needs to be trained.

3.6.1. Attention gate

A straightforward but efficient attention gate into our nested design to concentrate on areas that are pertinent to the target organ. The attention gate is examined in greater detail here. The gating signal is the initial input (g), which facilitates learning the succeeding information.

- The following input learning is facilitated using the first input (g) as a gating signal. From encoded features (f), the compelling features are chosen by the gating signal (g), and then, these features are transferred to the top decoder.
- Batch Norm (bg, bf) and CNN operation (Wg, Wf) are used for integrating these input data pixel by pixel.
- The divergence of the Gate's parameters and attention coefficient (α) is determined by selecting the activation function with an S-shaped sigmoid($\sigma^2(x) = \frac{1}{1+e^{(-x)}}$).
- A particular coefficient is used for multiplying the encoder features of each pixel, and the result can be obtained.

The segmentation task-related target region can be better learned by the attention gate. While the task-unrelated target area can be suppressed thanks to the attention gate's effective function selection function. For the feature selection phase, the attention gate is presented in (2).

$$F = \sigma_1[(W_f^T \times f + b_f) + (W_g^T \times g + b_g)] \quad (2)$$

F=feature selection process
Gating signal (g)
Encoded features (f)
W=network weight
α=attention coefficient
CNN operation=(W_g, W_f)
Batch norm=(b_g, b_f)

$$\alpha = \sigma_2(W_\theta^T \times F + b_\theta) \quad (3)$$

$$output = f \times \alpha \quad (4)$$

3.6.2. Attention-based nested U-Net

For medical image segmentation, an integrated network called ANU-Net is used. ANU-Net is the combination of the Nested U-Net architecture and Attention mechanism. The encoder delivers the contextual information, and the encoder's relevant layers gather information via the broad skip links.

Every decoder's convolutional block obtains two equally sized feature maps as inputs in case of several dense skip connections: the original feature maps are developed using the same depth residual links of previous attention gates. The features are reconstructed after all received feature maps are received and concatenated. The extracted ANU-Net feature map can be stated in words and $Y_{u,v}$ represent the convolutional block result. The sequence of the convolutional block is denoted by v, and u represent feature depth.

$$\begin{cases} \varphi\left[Y_{u-1,v}\right], v = 0 \\ \varphi\left[\sum_{k=0}^{v=1} A_g(Y_{u,k}), U_p(X_{u+l}, v-1)\right], v > 0 \end{cases} \quad (5)$$

The mean upsampling $Ag(Y_{u,k})$ and attention Gate $Up(Y_{u+1,v-1})$ are then selected. The indicator from a node in the uth layer concatenate $\sum_{k=0}^{u=1} Ag(Y_{u,k})$ $Y_u, k = 0$ *to* Y_v, $k = v-1$

S the attention gates' results

The decoder's convolution blocks are used to select the same-scale feature maps from the encoder. Inputs for this layer are the results of the j preceding blocks. The network transfer of encoder feature data is one of ANU-Net's significant developments.

3.6.3. Parameters optimization using FPOA

For loss function reduction, the network optimization method is used. The optimizer performance is evaluated by the most significant weight, such as learning rate and regularization. While Regularisation prevents the significant weighting elements from making accurate predictions, it prevents the model from overfitting. As a result, the classifier's capacity for generalization improves. FPOA optimization algorithm is used for the experiments.

The FPOA optimization techniques are used to optimize the variation in weights in the proposed network model. Self-pollination and cross-pollination are two different types of pollination. Cross-pollination is a biological process. The local search is represented by abiotic pollinators, while objects of global tracking are represented by biotic pollinators using levy flight. For determining abiotic and biotic pollination, the switching probability $P \in [0,1]$ is used. Where pollen i along vector e_i is indicated by the $e_i(t)$, and levy flight is denoted by L. The notation of L specifies levy flight, at iteration t, q^* shows the present best solution at iteration t. The flower consistency equation is depicted as (6):

$$e_i(t+1) = e_i(t) + L(e_i(t) - q^*) \quad (6)$$

Requirement: Number of search agents: k, dimension: d, Batch size: q, Number of iterations for optimization: t, hyperparameter evaluation
function: Fy, hyperparameters: M1,M2,M3,M4

Initialize Random Flower pollinator population. $e_i(i = 1,2,...k)$
Initialize a, A, B

Procedure: Sample a batch of training data
Determine the search consistency probability$p \in [0,1]$.
while the number of optimization iteration
for k=1 to m (m=flowers in the population)
if rand>p, use a Levy flight to determine global pollination
else
choose j and k among the obtained solution and perform local pollination using
$e_i(t+1) = e_i(t) + L(e_i(t) - q^*)$
End if
Obtain new solutions and evaluate their fitness
Check the new solution, if it is better to choose a new solution
Else retain the previous solution
Choose the first three search agents: $\lambda,\ \mu,\ \delta$
End if
End for
Update a, A, B
(M1, M2, M3, M4) = hypermeter evaluation function (Fy)
Update $\lambda,\ \mu,\ \delta$
End while
W&b $\leftarrow$ sgdm (F_y, M1, M2, M3, M4)
End Procedure

The convergence and accuracy of CNN are significantly dependent on the hyperparameter. Hyper-parameters for the network were chosen on the basis of CNN. For CNN training, the regularization coefficient, the number of epochs, and the learning rate are optimized. The weight updates are controlled by a velocity and the learning rate adjusts the gradient descent algorithm's speed. To update the network several times with the entire dataset, number of epochs are used. The regularization coefficient is used for avoiding over-fitting.

The algorithm provides details about hyperparameter optimization using FPOA. In this research, the segmentation process is initiated by the fully connected layer, which is the final layer. It exhibits high generalization capabilities for improving the classifier's accuracy.

4. RESULT AND DISCUSSIONS

This section compares the proposed method to existing state-of-the-art techniques and discusses the several measures of performance utilized for evaluating the model. The experimental evaluation is performed by using Python. The images have been standardized in size and resolution to fulfill the input requirements of each model. The SqueezeNet model classifies several age-related eye diseases. The AMD disease OCT images are segmented by developing the ANU-Net-FPOA model. The performance evaluation is performed by using the public image database.

4.1. Performance evaluation for classification

Whether the diagnosed disease is actually or falsely classified in the OCT images is determined by assessing each CNN's performance, with several evaluations further examined as follows. The cross-validation estimator is developed first for creating the confusion matrix. The proposed model is efficiently classified using a specific class to associate the model, and all data samples are included in the true positive (TP) indices. Additional examples are available for the true negative (TN) indices in the confusion matrix. These samples relate to other classes that have been successfully identified. In the uncertainty matrix, the false negative (FN) and false positive (FP) indices denote the classifier's estimated Number of incorrect samples.

The parameters of the confusion matrix determine the classifier's performance in the proposed model. The confusion matrix is used to assess performance measures for the accuracy of experimental analysis. By dividing the total values of the confusion matrix through the proportion of true positive and actual negative values, (7) defines accuracy as:

$$Accuracy(\%) = \frac{TP+TN}{TP+FN+TN+FP} \quad (7)$$

Similarly,

$$Sensitivity(Re\ c\ all) = \frac{TP}{TP+FN} \quad (8)$$

$$pecificity = \frac{TN}{TN+FP} \quad (9)$$

4.2. Experimental evaluation

Various classification tasks are used to test deep learning-based methods. The wet AMD, dry AMD, and healthy classes of images are classified using the proposed model analysis. All classification tasks are performed using the ANU-Net deep learning architecture and network parameters. It is tested using the available test data after being trained using the training data of each class. Figure 2 shows the proposed model's experimental results. The proposed model effectively segments the AMD disease's subretinal fluid (SRF) region.

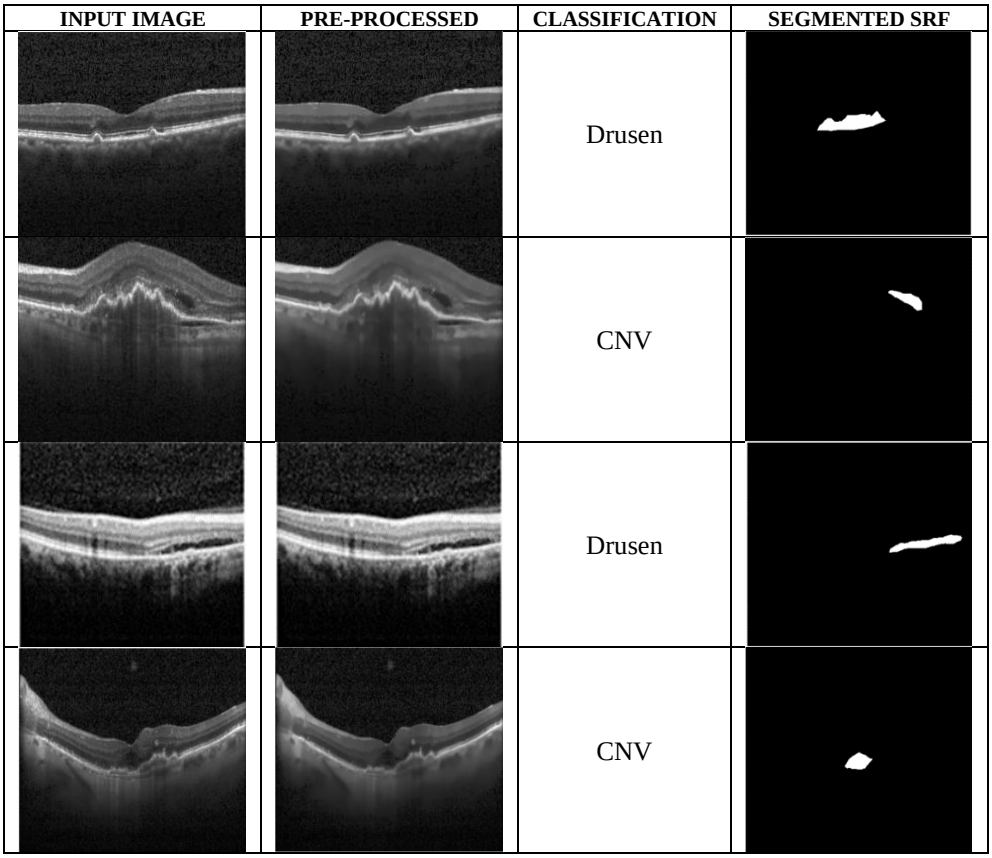

Figure 2. Experimental results

By conducting the training phase, the better results are achieved with learning rate of 0.01 and 26 epochs. For each period, the experiment analysis used 31 iterations. The accuracy and loss of multiple retinal disease classifications for training and validation are given in Figure 3. With an accuracy of 98.7%, training progress validation was performed. A timing of 1 min 54 s is employed throughout the entire training process to arrive at the final iteration. For the training process, the images were sent into the 224×224×3 input layer. The hyperparameters are selected to improve the validation accuracy during the training phase.

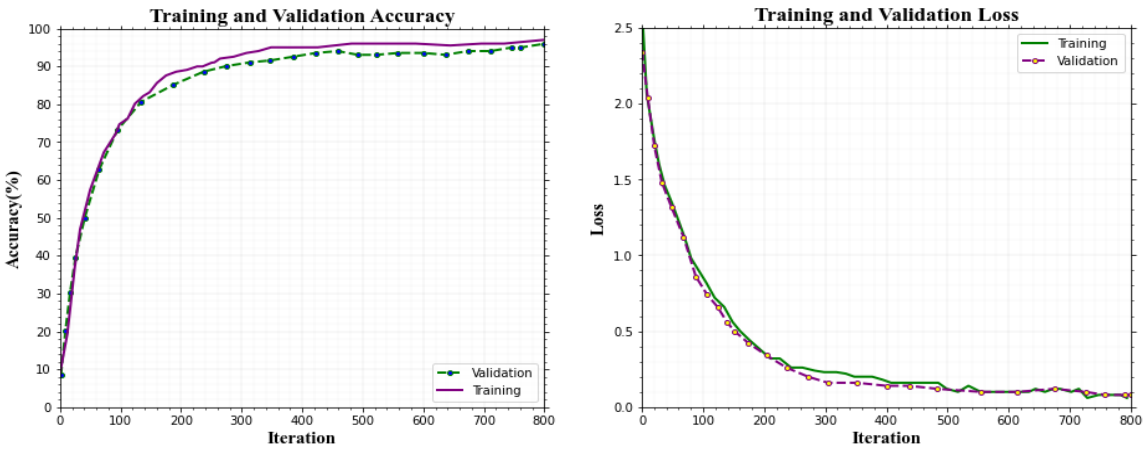

Figure 3. Accuracy and loss curve for training and validation of the proposed model.

The classification performance for healthy, dry AMD and wet AMD images is first assessed. 83484 OCT images were used to train the ANU-Net architecture. Each category has 250 images for the performance test. For each class, the effectiveness of the proposed model is assessed using the confusion matrix values. Accuracy, sensitivity, and specificity measurements are used to evaluate these values. Figure 4(a) displays the proposed model's confusion matrix. The ROC curve of the proposed model is given in Figure 4(b). The proposed model's performance results are shown in Table 1. This table shows the proposed model's accuracies, specificities, and sensitivities for each class. From the analysis, the classification of performance results is significantly improved by the proposed model. A total of 98.7% accuracy, 99.7% sensitivity, and 99.8% specificity were provided by the proposed algorithm. The class-wise performance is assessed using a validation set's images with small sample. The macular pathology classification is effectively done by the proposed deep learning model.

Table 1. Class-wise performance of the proposed method

Performance measures	Drusen (dry AMD)	CNV (wet AMD)	Normal
Sensitivity (%)	99.67	99.83	99.73
Specificity (%)	99.36	99.69	99.38
Accuracy (%)	98.91	98.63	99.12

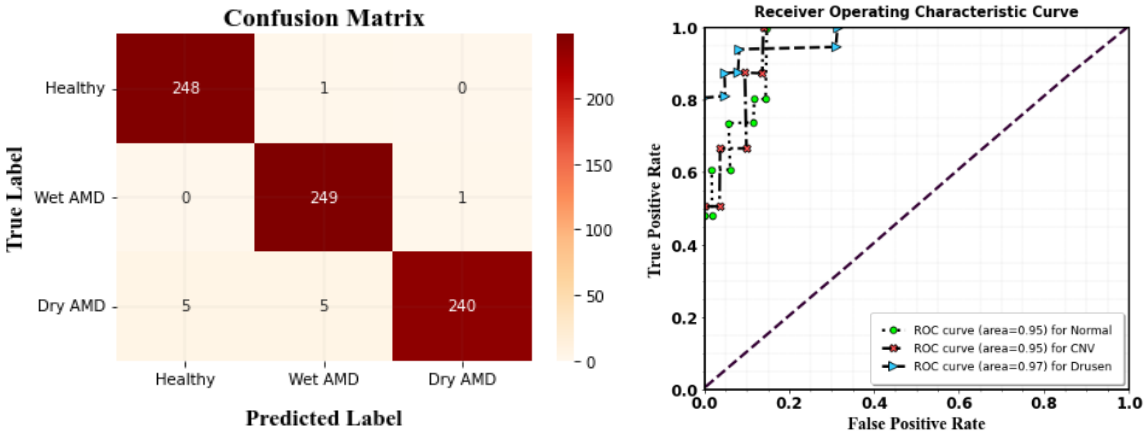

(a) (b)

Figure 4. Evaluation of proposed model for (a) confusion matrix multi-class classification and (b) ROC curve of multi-class classification

4.3. Comparison results

Table 2 provides a performance comparison, and the proposed method was contrasted with the existing techniques for identifying disorders like Drusen, CNV, and routine. While comparing the four different optimization methods to the proposed model, the proposed model effectively detects the retinal diseases and successfully segments the AMD disease images. The proposed ANU-Net model with an FPOA optimizer configuration provides the best results. The effectiveness of the proposed method is compared with the currently existing methods, such as CNN-root mean squared propagation (RMS prop), VGG-16-Stochastic gradient descent (SGD), ResNet-Adam, and InceptionV3-Adam. The proposed ANU-Net-FPOA model achieves better results and effectively identifies the multi-class retinal disease classification. In this research, the framework for the proposed ANU-Net network model is simple compared to the previous analysis.

Table 2. Performance comparison results

Models	Specificity (%)	Sensitivity (%)	Accuracy (%)
Inception V3	97.4	97.8	96.6
ResNet50	99.4	96.8	97.9
AlexNet	97.1	99.3	97.1
VGG-19	96.2	97.4	92.7
The proposed model (ANU-Net-FPOA)	99.8	99.7	98.7

The suggested approach achieves successful feature extraction from the diseases' inter-scale variability, which also enhances classification performance. The proposed method performs better for classifying macular disease than the existing methods. The proposed method achieves a 98.7% accuracy, 99.8% specificity and 99.7% sensitivity. The suggested model automatically detects and screens for retinal disorders with high accuracy for classification. The comparison of performance analysis is given in Figure 5.

The GAN-based model is examined by Yoo *et al*. [26] for OCT diagnosis. The deep learning-based GAN model achieves 92.10% accuracy for retinal disease classification. Pre-trained CNN models with the Grad-CAM technique were utilized by Daanouni *et al.* [27] to predict AMD. A custom CNN is retrained using transfer learning-based MobileNet for reliable OCT classification. The essential features in the images are highlighted by using Grad-CAM for effective prediction to demonstrate that this approach is feasible and this model achieves 80% accuracy. VGG19 model with Grad-CAM technique is proposed by Taibouni *et al.* [28] for OCT image classification, reaching 83.76% accuracy. The performance accuracy of the proposed ANU-Net with FPOA optimizer is higher than the MobileNet- Grad-CAM and VGG19- Grad-CAM approaches because the localization capability of a disease in an image by using Grad-CAM is very challenging.

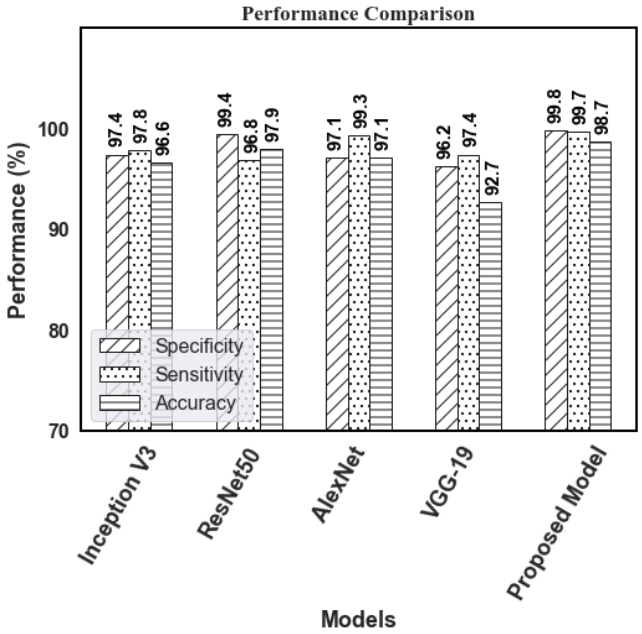

Figure 5. Performance analysis

5. ABLATION STUDY

No specific deep learning framework is required for the proposed ANU-Net-FPOA optimizer algorithm to perform well. Numerous experiments were compared with well-liked deep learning models such as VGG19 and ResNet50. It is discovered that the network's performance in ResNet50 or VGG16 is comparable in each instance. Table 2 presents the experimental findings. The table shows that the results achieved regarding the accuracy, sensitivity, and specificity utilize the 5-fold cross validation (CV) technique, using ResNet50 and VGG19 as the base models. Therefore, the choice of a deep pre-trained network does not affect the diagnostic accuracy of the ANU-Net-FPOA architecture.

Additionally, we have revealed that the optimization approach specifies the Number of parameters needed for these models. While the performance of the ANU-Net-based network is higher than that of the VGG-19-based network, we can see that the network using VGG19 has fewer parameters than the one using ResNet50 as the framework. Therefore, we selected ANU-Net as our base model for the proposed architecture to maximize the classification output and resource requirements.

6. CONCLUSION

Detecting retinal diseases using OCT images is a novel automatic technique we proposed in this research. The various retinal disorders are classified using the OCT images in the proposed model, such as CNV, Drusen, and routine. A publicly tested dataset (UCSD dataset) is used to test the diagnostic performance of the proposed model. First, retinal flattening, image cropping, and normalization are applied to the retinal OCT images to perform image pre-processing. Next, the SqueezeNet model is used to classify retinal diseases. Then the ANU-Net model was then used to segment the retinal OCT images. The FPOA is used to optimize the hyperparameters, and efficiency and accuracy are increased by using this optimizer. The diseased image was more accurately identified by the proposed ANU-Net-FPOA model with an accuracy of 98.7% than other approaches. The results demonstrated that this approach could discriminate between CNV, drusen, and normal with high precision, sensitivity, and specificity. The preliminary retinal screening is effectively done by the proposed method in eye clinics because of these characteristics. These features help ophthalmologists design the proper treatments and make decisions on diagnostics. The proposed CNN can be used in real time since it is less complex and has fewer learnable parameters.

REFERENCE

[1] F. Li *et al.*, "Deep learning-based automated detection of retinal diseases using optical coherence tomography images," *Biomedical Optics Express*, vol. 10, no. 12, p. 6204, Nov. 2019, doi: 10.1364/boe.10.006204.

[2] J. Y. Choi, T. K. Yoo, J. G. Seo, J. Kwak, T. T. Um, and T. H. Rim, "Multi-categorical deep learning neural network to classify retinal images: a pilot study employing small database," *PloS one*, vol. 12, no. 11, p. 0187336, Nov. 2017, doi: 10.1371/journal.pone.0187336.

[3] Y. Deng *et al.*, "Age-related macular degeneration: epidemiology, genetics, pathophysiology, diagnosis, and targeted therapy," *Genes & diseases*, vol. 9, no. 1, pp. 62–79, Jan. 2022, doi: 10.1016/j.gendis.2021.02.009.

[4] S. A. Tuncer, A. Ç\inar, and M. F\irat, "Hybrid CNN based computer-aided diagnosis system for choroidal neovascularization, diabetic macular edema, drusen disease detection from OCT imagess," *Traitement du Signal*, vol. 38, no. 3, pp. 673–679, Jun. 2021, doi: 10.18280/ts.380314.

[5] G. N. Girish, B. Thakur, S. R. Chowdhury, A. R. Kothari, and J. Rajan, "Segmentation of intra-retinal cysts from optical coherence tomography images using a fully convolutional neural network model," *IEEE Journal of Biomedical and Health Informatics*, vol. 23, no. 1, pp. 296–304, Jan. 2019, doi: 10.1109/jbhi.2018.2810379.

[6] Q. Ji, W. He, J. Huang, and Y. Sun, "Efficient deep learning-based automated pathology identification in retinal optical coherence tomography images," *Algorithms*, vol. 11, no. 6, p. 88, Jun. 2018, doi: 10.3390/a11060088.

[7] A. M. Alqudah, "AOCT-NET: a convolutional network automated classification of multi-class retinal diseases using spectral-domain optical coherence tomography images," *Medical & Biological Engineering & Computing*, vol. 58, no. 1, pp. 41–53, Nov. 2019, doi: 10.1007/s11517-019-02066-y.

[8] P. T. A. Bui *et al.*, "Fundus autofluorescence and optical coherence tomography biomarkers associated with the progression of geographic atrophy secondary to age-related macular degeneration," *Eye*, vol. 36, no. 10, pp. 2013–2019, Aug. 2021, doi: 10.1038/s41433-021-01747-z.

[9] S. A. P, S. Kar, G. S, V. P. Gopi, and P. Palanisamy, "OctNet: a lightweight cnn for retinal disease classification from optical coherence tomography images," *Computer Methods and Programs in Biomedicine*, vol. 200, p. 105877, Mar. 2021, doi: 10.1016/j.cmpb.2020.105877.

[10] Z. Chen, D. Li, H. Shen, H. Mo, Z. Zeng, and H. Wei, "Automated segmentation of fluid regions in optical coherence tomography B-scan images of age-related macular degeneration," *Optics & Laser Technology*, vol. 122, p. 105830, Feb. 2020, doi: 10.1016/j.optlastec.2019.105830.

[11] B. I. Dodo, Y. Li, D. Kaba, and X. Liu, "Retinal layer segmentation in optical coherence tomography images," *IEEE Access*, vol. 7, pp. 152388–152398, 2019, doi: 10.1109/access.2019.2947761.

[12] A. Alqudah, A. M. Alqudah, and M. AlTantawi, "Artificial intelligence hybrid system for enhancing retinal disease classification using automated deep features extracted from OCT images," *International Journal of Intelligent Systems and Applications in Engineering*, vol. 9, no. 3, pp. 91–100, Sep. 2021, doi: 10.18201/ijisae.2021.236.

[13] I. K. Muftuoglu, H. L. Ramkumar, D.-U. Bartsch, A. Meshi, R. Gaber, and W. R. Freeman, "Quantative analysis of the inner retinal Layer thicknesses in age-related macular degeneration using corrected optical coherence tomography segmentation," *Retina*,

vol. 38, no. 8, pp. 1478–1484, Aug. 2018, doi: 10.1097/iae.0000000000001759.
[14] Y. Derradji, A. Mosinska, S. Apostolopoulos, C. Ciller, S. De Zanet, and I. Mantel, "Fully-automated atrophy segmentation in dry age-related macular degeneration in optical coherence tomography," *Scientific Reports*, vol. 11, no. 1, pp. 1–11, Nov. 2021, doi: 10.1038/s41598-021-01227-0.
[15] W.-D. Vogl, H. Bogunović, S. M. Waldstein, S. Riedl, and U. Schmidt-Erfurth, "Spatio-temporal alterations in retinal and choroidal layers in the progression of age-related macular degeneration (AMD) in optical coherence tomography," *Scientific Reports*, vol. 11, no. 1, pp. 1–11, Mar. 2021, doi: 10.1038/s41598-021-85110-y.
[16] D. Xu *et al.*, "Long-term progression of type 1 neovascularization in age-related macular degeneration using optical coherence tomography angiography," *American Journal of Ophthalmology*, vol. 187, pp. 10–20, Mar. 2018, doi: 10.1016/j.ajo.2017.12.005.
[17] T. Tsuji *et al.*, "Classification of optical coherence tomography images using a capsule network," *BMC Ophthalmology*, vol. 20, no. 1, pp. 1–9, Mar. 2020, doi: 10.1186/s12886-020-01382-4.
[18] L. Huang, X. He, L. Fang, H. Rabbani, and X. Chen, "Automatic classification of retinal optical coherence tomography images with a layer-guided convolutional neural network," *IEEE Signal Processing Letters*, vol. 26, no. 7, pp. 1026–1030, Jul. 2019, doi: 10.1109/lsp.2019.2917779.
[19] A. Arrigo *et al.*, "Advanced optical coherence tomography angiography analysis of age-related macular degeneration complicated by the onset of unilateral choroidal neovascularization," *American Journal of Ophthalmology*, vol. 195, pp. 233–242, Nov. 2018, doi: 10.1016/j.ajo.2018.08.001.
[20] X. He, L. Fang, H. Rabbani, X. Chen, and Z. Liu, "Retinal optical coherence tomography image classification with label smoothing generative adversarial network," *Neurocomputing*, vol. 405, pp. 37–47, Sep. 2020, doi: 10.1016/j.neucom.2020.04.044.
[21] A. Thomas, P. M. Harikrishnan, A. K. Krishna, P. Palanisamy, and V. P. Gopi, "Automated detection of age-related macular degeneration from OCT images using multipath CNN," *Journal of Computing Science and Engineering*, vol. 15, no. 1, pp. 34–46, Mar. 2021, doi: 10.5626/jcse.2021.15.1.34.
[22] K. Alsaih, M. Z. Yusoff, T. B. Tang, I. Faye, and F. Mériaudeau, "Deep learning architectures analysis for age-related macular degeneration segmentation on optical coherence tomography scans," *Computer Methods and Programs in Biomedicine*, vol. 195, no. 1, p. 105566, Oct. 2020, doi: 10.1016/j.cmpb.2020.105566.
[23] J. H. Tan *et al.*, "Age-related macular degeneration detection using deep convolutional neural network," *Future Generation Computer Systems*, vol. 87, no. 1, pp. 127–135, Oct. 2018, doi: 10.1016/j.future.2018.05.001.
[24] A. Serener and S. Serte, "Dry and wet age-related macular degeneration classification using oct images and deep learning," in *2019 Scientific meeting on electrical-electronics & biomedical engineering and computer science (EBBT)*, Apr. 2019, pp. 1–4, doi: 10.1109/ebbt.2019.8741768.
[25] S. P. K. Karri, D. Chakraborty, and J. Chatterjee, "Transfer learning based classification of optical coherence tomography images with diabetic macular edema and dry age-related macular degeneration," *Biomedical Optics Express*, vol. 8, no. 2, pp. 579–592, Jan. 2017, doi: 10.1364/boe.8.000579.
[26] T. K. Yoo, J. Y. Choi, and H. K. Kim, "Feasibility study to improve deep learning in OCT diagnosis of rare retinal diseases with few-shot classification," *Medical & Biological Engineering & Computing*, vol. 59, no. 2, pp. 401–415, Jan. 2021, doi: 10.1007/s11517-021-02321-1.
[27] O. Daanouni, B. Cherradi, and A. Tmiri, "Automatic detection of diabetic retinopathy using custom CNN and grad-cam," in *Advances on Smart and Soft Computing*, Springer Singapore, 2020, pp. 15–26.
[28] K. Taibouni, A. Miere, A. Samake, E. Souied, E. Petit, and Y. Chenoune, "Choroidal neovascularization screening on OCT-angiography Choriocapillaris images by convolutional neural networks," *Applied Sciences*, vol. 11, no. 19, p. 9313, Oct. 2021, doi: 10.3390/app11199313.

BIOGRAPHIES OF AUTHORS

Gilakara Muni Nagamani is a PhD full-time Research Scholar in the School of Computer Science and Engineering from VIT-AP University, Amaravati. The author was awarded B.Tech and M.Tech degrees from JNTU Anantapur and had around 5 years of Teaching experience and 3 years of Industrial experience. Her Research Interests include Image Processing, Deep Learning and Machine Learning. She can be contacted at email: gmuninagamani.vit@gmail.com.

Dr. Theerthagiri Sudhakar received his B.E and M.E. degrees in computer science and engineering discipline in the years 2002 and 2005 respectively. He received his PhD from the Faculty of Information and Communication Engineering, Anna University, Chennai in 2019. He is currently working as an Associate Professor, at the School of Computer Science and Engineering, VIT-AP University, Amravati, Andhra Pradesh, India. He has 17 years of teaching experience and 8 years of research experience. He has published a number of research articles in various reputed international journals and conferences. His research interests include Cryptography, Network Security, Design of security protocols, Algorithms and Cyber Security, Image Processing, and Deep Learning. He can be contacted at email: drsudhakar.vitap@gmail.com.